INTEGRATION OF A BOREHOLE THERMAL ENERGY STORAGE MODEL INTO A TECHNO-ECONOMIC OPTIMIZATION TOOL FOR DISTRICT HEATING

Paul Mex[1]*, Maximilian Sporleder[1]

[1]Fraunhofer Research Institution for Energy Infrastructures and Geothermal Systems (IEG), Cottbus, Germany

*Paul Mex: paul.mex@ieg.fraunhofer.de

ABSTRACT

Renewable district heating systems are likely to play a key role in the decarbonization process of the heating sector in Germany and northwestern Europe. The seasonal fluctuation of supply and demand calls for large seasonal thermal energy storages, with borehole thermal energy storages (BTES) coupled to heat pumps being currently among the most promising concepts. In this paper, the automated connection of a complex g-function-based BTES model with a mixed integer linear programming (MILP) techno-economical optimization tool for topologically discretized district heating systems is demonstrated. This allows the optimal sizing of both the BTES field layout and the depth including a detailed simulation of the BTES temperatures using the open-source *Python* tool *GHEDesigner*. A small district heating system with six energy consumers and solar thermal energy as the main energy source is simulated and optimally designed, containing a BTES or a pit thermal energy storage (PTES) enabling a comparison of the competing storage technologies resulting in similar heat generation costs for both systems. A sensitivity analysis identifies dependencies of the BTES and PTES and compares them for different scenarios. Since the heat pump coupled to the BTES has a small coefficient of performance, its electricity consumption is three times higher and a BTES system depends strongly on the electricity price due to high operational expenditures. Its increase of the heat generation costs over a changing electricity price are 1.4 times stronger than in case of a PTES system. However, compared to a PTES, because of geothermal gains of the BTES and the conversion of much power to heat in the heat pump, the BTES capacity can be smaller by about 41 % and the dimension of the solar thermal field by 51 % resulting in 19 % lower investments. PTES depend strongly on the land area costs as opposed to BTES whose area above them can still be used making them attractive for urban areas. These and further findings are a contribution to the controversially led discussion whether BTES can compete with other large storage technologies.

1 INTRODUCTION

The Paris Agreement, established by the United Nations (UNFCCC, 2015), has the objective of reducing greenhouse gas emissions in order to limit global warming. The agreement sets a target to keep the global average temperature increase well below 2 °C and to make efforts to limit it to 1.5 °C. However, since 1981, the earth's temperature has been rising at a rate of 0.18 K per decade, and the hottest ten years on record have occurred within the past 13 years (Lindsey and Dahlmann, 2023). In Germany, roughly 30 % of the final energy consumption is caused by space heating (25 %) and hot water demand (5 %). With process heat, 50 % of Germany's total final energy consumption is associated with heat (AGEB, 2016; BMWK, 2021). This considerable sector still has a long way to go in achieving decarbonization. Fossil fuels account for 80 % of the energy supplied by German district heating networks (DHN) (BMWK, 2019). It is inevitable that DHNs have to be decarbonized through the integration of renewable energy systems. By achieving this, district heat (DH) might play a key role in decarbonizing the overall heat supply of northwestern European countries, and its share in the energy mix is likely to increase (Lund *et al.*, 2010; Connolly *et al.*, 2014). One promising strategy is the implementation of large-scale central solar thermal collector (STC) fields (Schmidt *et al.*, 2004). To

https://doi.org/10.52202/077185-0080

address the seasonal fluctuations in the energy supply, storage systems need to be integrated into these DHS. Currently, only sensible thermal energy storage (TES) systems are available and economically viable for large applications, unlike latent and chemical heat storage methods (Pinel *et al.*, 2011). Sensible TES can be categorized into different types, including borehole (BTES), pit (PTES), tank (TTES), and aquifer (ATES) thermal energy storages. The economic feasibility of BTES systems is still a topic of debate. Welsch (2019) argues that the initial investments for a BTES are very high, but specific costs (relating to the storage capacity) are comparably low, aligning with the findings of Mangold *et al.* (2012). However, in a review study on seasonal TES, Yang *et al.* (2021) suggest that BTES systems are rather expensive compared to other technologies such as PTES. However, the storages were integrated at different locations, sometimes with and sometimes without a heat pump coupled to the storage. These fundamentally different circumstances make a comparison difficult. Hence, our aim is to complement the research conducted by Yang *et al.* (2021) by examining the integration of PTES and BTES through a small-scale case study. We assess which storage type might be applicable under different circumstances in terms of economic feasibility in the future (2030). The techno-economic performance of a BTES and a PTES is compared. For optimization purposes of DHS, MILP is a powerful approach. In this study, the automated connection of a non-linear BTES model with a MILP techno-economical optimization tool for topologically discretized DHS is demonstrated. This work will focus on the BTES integration and modelling. The aforementioned techno-economical DHS optimization tool has been presented by Sporleder *et al.* (2023), including a detailed PTES model.

1.1 State-of-the-art

BTES are composed of several ground heat exchangers (GHE). The GHEs are vertical boreholes equipped with a closed-loop piping system, typically U-, double-U- or concentric pipes, with water or glycol-water mixtures serving as the working fluid circulating in them. Heat is then transferred from the soil to the working fluid and vice versa mainly by conduction. In order to simulate this heat transfer between a GHE and the ground, analytical functions (often called g-functions) are promising and widely used, especially on early design stages. Alternative numerical simulation approaches have the disadvantage of high computational time (Li and Lai, 2015). The historically first g-function was the analytical solution of a heat transfer problem of an infinite line source (ILS) in an infinitely expanded solid medium, solved by Carslaw and Jaeger (1959) in the 20th century (Banks, 2015). Further analytical line source models have been developed over the years in order to take other effects like a high groundwater flow into account. An overview over these more refined line source models is given by Li and Lai (2015). The linear spatial superposition of the g-functions of several single GHEs allows a detailed simulation of GHE fields. Eskilson and Claesson developed with the *Superposition Borehole Model* (*SBM*) a closed-source computer program to numerically pre-calculate g-functions for entire GHE fields (with a given layout meaning the positioning of the GHEs) and store them in libraries (Eskilson, 1987; Eskilson and Claesson, 1988). This approach is used in commercial software like *EED* (Blocon AB, 2022) allowing the optimization of the GHE depth. An alternative open-source approach has been introduced with the *Python* package *pygfunctions* (Cimmino and Cook, 2022). It still allows building pre-calculated libraries as well as fast live-calculation of g-functions of even custom irregular borehole field shapes. *pygfunctions* enabled the development of open-source GHE field optimization tools like *GHETool* (Peere and Blanke, 2022) and *GHEDesigner* (Spitler *et al.*, 2022), the latter being the only tool (of open- and closed-source tools) which can optimize both the depth and the layout of the field. For cases in which the field layout is already known, the g-functions can be directly implemented in MILP programs in order to optimize the GHE depth or other variables of isolated GHE field models coupled to heat pumps (Paly *et al.*, 2012; Beck *et al.*, 2013), or BTES with a heat pump integrated in small energy systems including one building and several supply units (Kümpel *et al.*, 2022) or integrated in small DHS (Gabrielli *et al.*, 2020). In the contrary, the combination of an unknown GHE layout (or number of GHEs) and an unknown depth leads to a non-linearity. Such cases are usually not addressed in the scientific literature even though during any design process both the GHE layout and the depth have to be designed. This work will address this research gap by combining the DHS MILP model and a BTES model using the *GHEDesigner*. This will enable the optimization of design and operation of a BTES integrated in a large energy system, namely a DHS incorporating an STC field, a BTES heat pump and several consumers as depicted in Figure 1. Both the supply and demand units on the one

https://doi.org/10.52202/077185-0080

hand, and the grid on the other hand are simulated during the optimization. The coupling of the *GHEDesigner* to the DHS MILP model will enable the optimization of both the GHE field layout and the depth. This allows the detailed answering of further research questions such as the aforementioned comparison of BTES and PTES on a large system scale being the second main research gap addressed in this paper. Additionally, this work includes a sensitivity analysis to examine key parameters and their impact on the techno-economic performance of the BTES. After this introduction and review of the state-of-the-art of BTES modelling, the methods applied in this work will be presented. In the results section, the case study will be evaluated and a detailed techno-economical comparison of a DHS equipped with a BTES or a PTES respectively will be presented. The results of a sensitivity analysis with respect to parameters such as the electricity price, drilling costs, the ground thermal conductivity and the land area price are shown. Finally, the results and findings will be discussed and concluded.

2 METHODS AND DATA

The BTES model will be integrated into an existing DHS optimization tool (Sporleder *et al.*, 2023). The model is structured into various components, including pipes, nodes, consumers, producers, storages, technology constraints, and the objective function aiming to minimize operational (opex) and capital expenditures (capex) (McKenna *et al.*, 2019). In DHS planning, often the network (Bordin *et al.*, 2016) or the supply system (Wirtz *et al.*, 2021) are designed and optimized separately. Our MILP model, written in *Python*, focusses on optimizing the design of the supply system and the network's operation regarding mass flows and temperatures without changing the network's topology. The operational optimization over one year is crucial for taking the storages' seasonal effects into account (Kotzur *et al.*, 2018). To satisfy the linearity criterion, the mass flow within the pipes is estimated a priori (Sporleder *et al.*, 2023). The model can be solved using solvers such as the Gurobi solver (Gurobi Optimization LL., 2023). The objective function aims to minimize the cost function $\min\left(f^{\mathrm{opex,var}}, g^{\mathrm{opex,fix}}, h^{\mathrm{capex}}\right)$. $f^{\mathrm{opex,var}}$ are the variable opex for storages or energy converters including costs for energy carriers, maintenance and repair and $g^{\mathrm{opex,fix}}$ are the fixed opex for storages or energy converters and include costs for operation, maintenance and repair as well. h^{capex} denote the investment costs. All these costs are calculated according to VDI (2012) with data from the Danish Energy Agency (2022) for the year 2030, see section 2.3. A ten-year time horizon based on a one-year optimization in 24 h timesteps with an conservatively assumed interest rate of 6 % (ECB European Central Bank, 2024), calculating the annuity factor α with equation (4) in VDI (2012), is implemented.

2.1 Thermal Calculation and Integration of the BTES model

To incorporate the BTES model into the DHS optimization tool, a simplified storage model based on an energy balance is used. This simplified storage system is defined solely by an energy balance rule. The algorithm is designed to determine the optimal heat flow entering $\left(\dot{Q}^{\mathrm{in}}_{k=\mathrm{BTES},t}\right)$ and leaving $\left(\dot{Q}^{\mathrm{out}}_{k=\mathrm{BTES},t}\right)$ the GHE field serving as the thermal storage. The resulting

$$\dot{Q}^{\mathrm{res}}_{k=\mathrm{BTES},t} = \dot{Q}^{\mathrm{out}}_{k=\mathrm{BTES},t} - \dot{Q}^{\mathrm{in}}_{k=\mathrm{BTES},t} \text{ for } t \in Z^{\mathrm{time}} \tag{1}$$

is applied to the GHE field and can be passed to the BTES model. The energy level of the storage k at the time t is

$$E_{k,t} = E_{k,t-1} + \Delta t\left(\dot{Q}^{\mathrm{in}}_{k,t} - \dot{Q}^{\mathrm{out}}_{k,t} - \dot{Q}^{\mathrm{loss}}_{k,t}\right) \text{ for } t \in Z^{\mathrm{time}}, k \in Z^{\mathrm{stor}}. \tag{2}$$

Z^{time} denotes the time set, Z^{stor} the set of all storages. As opposed to the PTES, in the case of a BTES, the losses per time step Δt are set to $\dot{Q}^{\mathrm{loss}}_{k=\mathrm{BTES},t} = 0$ kW. This will lead to a balanced profile of $\dot{Q}^{\mathrm{res}}_{k=\mathrm{BTES},t}$ and of the temperature profiles of the soil and working fluid in the BTES model. A BTES is not only a storage, but also a geothermal heat source. Schmidt and Sørensen (2018) discuss this and the partly misleading character of the concept of storage efficiency regarding BTES. $\dot{Q}^{\mathrm{loss}}_{k=\mathrm{BTES},t} = 0$ kW means, that all thermal losses are compensated by geothermal gains. Examples of such common cases can be

https://doi.org/10.52202/077185-0080

found in the *EED*-Tutorials (EED, 2019) and could rather be called a constraint than an assumption. Additionally, a cyclic condition for both storages has been implemented with $E_{k\in Z^{\mathrm{stor}},t=0} = E_{k\in Z^{\mathrm{stor}},t=\mathrm{end}}$. The BTES is dimensioned with

$$\dot{Q}_k^{\mathrm{nom}} \leq \dot{q}_k^{\mathrm{nom,GHEs}} \cdot h_k \cdot z_k \text{ for } k \in Z^{\mathrm{BTES}}, \tag{3}$$

where the nominal dimension is $\dot{Q}_{k\in Z^{\mathrm{BTES}}}^{\mathrm{nom}} \leq \max\left(\dot{Q}_{k\in Z^{\mathrm{BTES}},t\in Z^{\mathrm{time}}}^{\mathrm{res}}\right)$ from equation (1) and $\dot{q}_k^{\mathrm{nom,GHEs}}$ the specific nominal heat flow rate of a GHE in Wm^{-1}. z_k and h_k denote the number of GHEs and their depth. The BTES investment costs are

$$C_k^{\mathrm{inv}} \leq h_k \cdot z_k \cdot c_k^{\mathrm{drill}} \text{ for } k \in Z^{\mathrm{BTES}}, \tag{4}$$

where c_k^{drill} are the specific drilling costs in $€\mathrm{m}^{-1}$ being the main investment cost driver regarding the BTES (see section 2.3). For the BTES, we assumed a required space of $100\ \mathrm{m}^2$ for technical equipment like the heat pump. The space above the BTES can still be used and is in this model not associated with any costs. The required space for the PTES is directly calculated with a piece-wise function from Sporleder *et al.* (2023). The coefficient of performance COP of the heat pump discharging the PTES or BTES is calculated based on the Carnot efficiency (Baehr and Kabelac, 2006) with a quality grade of 0.4 for air source heat pumps and 0.5 for all other heat pumps. For the PTES, the model by Schütz *et al.* (2016) is used. The STC field is dimensioned by

$$\dot{Q}_{k,t}^{\mathrm{conv}} \leq \mu_{k,t} A_k \gamma_{k,t} \text{ for } t \in Z^{\mathrm{time}}, k \in Z^{\mathrm{solar}}, \tag{5}$$

where $\mu_{k,t}$ is the collector's efficiency, A_k the collector's area, γ_t the solar radiation and Z^{solar} the set of all STC fields. $\mu_{k,t}$ depends on the grid supply temperature $T_{k,t}^{\mathrm{sup}}$ and is as in Sporleder *et al.* (2024)

$$\mu_{k,t} = -2.43 \cdot 10^{-5} \cdot \left(T_{k,t}^{\mathrm{sup}}\right)^2 + 1.075 \cdot 10^{-2} \cdot T_{k,t}^{\mathrm{sup}} - 3.241 \cdot 10^{-1} \cdot T_{k,t}^{\mathrm{sup}} \quad \text{for } t \in Z^{\mathrm{time}}, k \in Z^{\mathrm{solar}}. \tag{6}$$

Regarding the integration of the BTES model in the design process, first the DHS model including the simplified storage model (equation (1) to (4)) is simulated. At first, parameters in these equations are estimated. Since the BTES model seeks to use the maximum possible borehole depth $h_{\max}$, it is at first $h_k = h_{\max}$. $\dot{q}_k^{\mathrm{nom,GHEs}}$ is estimated (see section 2.3), z_k can then be calculated within the optimization. The $COP_{k\in Z^{\mathrm{HP,BTES}},t}$ of the BTES heat pump is estimated for the initial simulation as well (see section 2.3). After this first simulation, $\dot{Q}_{k=\mathrm{BTES},t}^{\mathrm{res}}$ is passed to the BTES model, the *GHEDesigner*, calculating the optimal GHE field layout (including z_k and h_k), $\dot{q}_k^{\mathrm{nom,GHEs}}$ and the BTES field working fluid temperature influencing $COP_{k\in Z^{\mathrm{HP,BTES}},t}$. These values are fed back to the DHS model. An iterative loop is implemented for the case, that the deviation of $\dot{q}_{k\in Z^{\mathrm{BTES}}}^{\mathrm{nom,GHEs}}$ and $COP_{t,k\in Z^{\mathrm{HP_{BTES}}}}$ before and after the DHS model is greater 6 %. The *GHEDesigner* has been chosen since it is the only tool which can optimize both the depth and the layout of the field. In early design stages, often a maximum target depth is known as well as a maximum available field area, but not the GHE field layout. Since this layout is unknown, the g-function (depending on h_k and z_k) cannot be included as a linear function in the MILP model which is why a decoupling of the DHS and the BTES model and an iterative optimization scheme is chosen. Furthermore, this decoupling allows the consideration of the different time horizons of both models. DHS are simulated over typically one year, BTES however over several (up to 30) years to account for long term effects on the ground temperature. *GHEDesigner* is open-source and written in *Python* which facilitates the integration into the existing model and scheme.

https://doi.org/10.52202/077185-0080

2.2 Case Study for the Techno-Economic Analysis of Seasonal Storages in District Heating Systems

This paper presents a simulation of a small DH grid with six consumers. The grid's dynamic supply temperature varies between 60 °C in summer and 80 °C in winter, with peaks of up to 90 °C. The combined heat demand of all consumers is 4.24 MWh. Figure 1 illustrates the layout of the consumers and the production unit including an STC field and a BTES system consisting of a GHE field and a large-scale heat pump. The STC field can directly supply the grid or charge the BTES (or do both simultaneously). The heat pump increases the temperature of the heat flow exiting the GHE field. Alternatively, a PTES could replace the BTES, with the only difference being a water-filled pit instead of a BTES field as the storage component. In section 3.1, the case of a BTES design will be compared to the PTES technology.

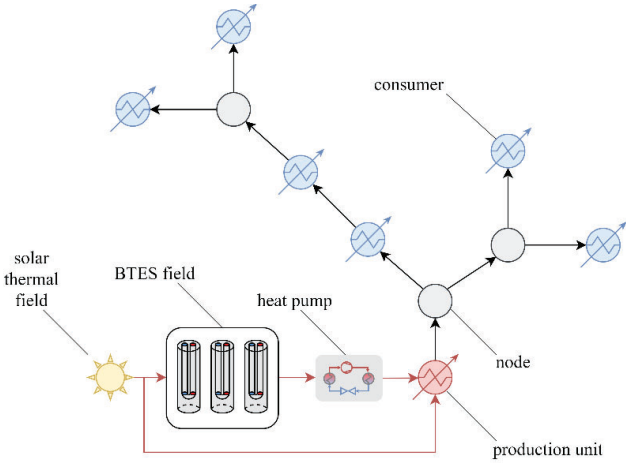

Figure 1: Fictional small DHS grid with a BTES as the seasonal storage. When comparing the BTES and PTES, the storage in this graphic is replaced, all other components remain.

2.3 Parameter and Model Initialization

To initialize the optimization model, various parameters for the BTES/GHE field model and parameters for the DHS optimization model are required. For the GHE field model, physical parameters related to the soil, working fluid, and borehole are primarily needed, taken from example 5 from the *EED*-Tutorials (EED, 2019). A thermal conductivity of the soil of $\lambda_S = 2.5\ \mathrm{Wm^{-1}K^{-1}}$ has been chosen being a typical value e.g. for wet sand (Grünert *et al.*, 2009; SenStadt, 2018). The techno-economic data such as the specific capex, variable, and fixed opex, efficiencies, part-load, technical lifetime, and energy carrier (electricity) is obtained from the Danish Energy Agency (2022) for the year 2030. Information on the PTES's capex and its geometry was taken from Xiang *et al.* (2022). The energy prices time series with an average of 5.44 ct $\mathrm{kW^{-1}h^{-1}}$ and their development was assumed as by Pfluger *et al.* (2023). The weather data is obtained by the European Commission (2016). Note, that for the BTES heat pump a device with two stages is automatically chosen due to the high temperature delta. This leads to higher specific heat pump investments compared to the PTES. The fix opex for the PTES pit or the BTES GHE field ($c^{\mathrm{PTES\backslash GHEs,opex,fix}}$) are assumed to be equal for both. Usually, $c^{\mathrm{GHEs,opex,fix}}$ is considered negligible. The assumption of a $c^{\mathrm{GHEs,opex,fix}}$ may slightly overestimate the BTES costs. Among all the costs associated with the GHE field, the specific drilling costs $\left(c^{\mathrm{drill}}\right)$ have the greatest impact and are often the only costs considered. Reviewing the existing literature regarding c^{drill}, an assumption of $c^{\mathrm{drill}} = 100\ €\mathrm{m^{-1}}$ seems appropriate (Robert and Gosselin, 2014; Blum *et al.*, 2011; Florides *et al.*, 2013). The impact of c^{drill} will be investigated in a sensitivity analysis in section 3.4. Only maximum depths of up to $h_{\max} = 250$ m are considered. The initial estimation of the nominal heat flow of the GHEs ($\dot{q}^{\mathrm{nom,GHEs}}_{k\in Z^{\mathrm{BTES}}}$ in equation (3)) can be obtained using common tabular values based on ground properties (VDI, 2010). Additionally, the COP for the initial DHS simulation can be calculated based on an estimated sinusoidal function of the temperature of the working fluid in the BTES $T_{\mathrm{f,init}}(t)$ with

https://doi.org/10.52202/077185-0080

a minimum of 3 °C at the start of the year, a maximum of 21 °C at $t = 0.5$ a and a frequency of 1 a^{-1} . The specific land costs are $c^{area} = 15$ €m^{-2} being comparably low and applicable for locations with a high land area availability. This parameter is part of the sensitivity analysis as well. More information on the model and its parameters can be found in a study by Sporleder *et al.* (2023).

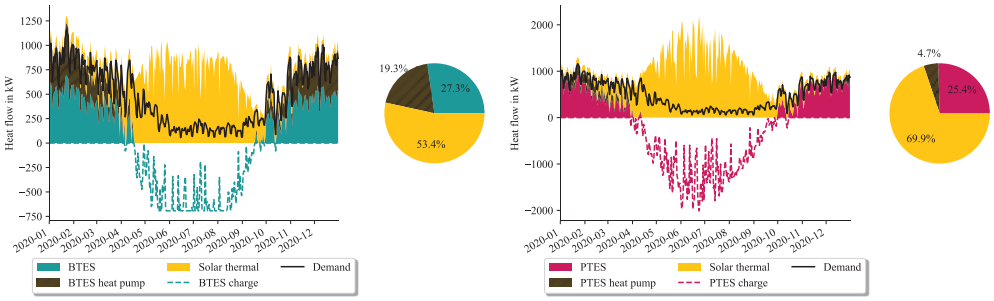

(a) (b)

Figure 2: Heat flows of a small DHS with six demand units and (a) a BTES or (b) a PTES system calculated by the DHS optimization program. The profiles of the STC field, BTES/PTES and their respective heat pumps are stacked. The pie charts show the fractions of the total energy fed into the grid per component.

3 RESULTS

3.1 Comparison of a Baseline Case of an Optimized DHS with a BTES or PTES

Figure 2 shows all supplying heat flows going into the grid, the demand profile (being the same in both cases) and the heat flow charging the BTES or PTES. Both cases, with a BTES or a PTES, are initialized as presented in section 2.3. Even though the PTES has a higher capacity, the pie charts in Figure 2 indicate, that the fractions of total energy supplied by the BTES or PTES storage are the same with around 25 %. This is due to the losses of the PTES. A second difference in Figure 2 is, that the BTES heat pump has a much higher fraction than for the PTES. This is caused by the much lower COP of the BTES heat pump due to the high temperature difference between storage and grid temperature. In the BTES heat pump, much electric energy is converted into heat. This leads consequently to less usage of solar thermal energy in the case of the BTES and a smaller STC area. For the BTES, the COP is $2.26 \leq COP \leq 3.56$, while for the PTES it is $2.77 \leq COP \leq 30$. In the summer, the PTES temperature even exceeds the grid temperature for several weeks, indicating that the heat pump is not needed and the energy can be directly supplied to the grid.

Table 1: Results and comparison of a BTES and a PTES system integrated in a small DHS

Device	Parameter	Unit	BTES	PTES
Entire supply system	Heat Generation Cost	ct $kW^{-1}h^{-1}$	22.51	22.22
	Total Investment $capex_{tot}$	M€	5.94	7.31
BTES field / PTES pit	$\dot{Q}_{nom,in}$	kW	693	2010
	$\dot{Q}_{nom,out}$	kW	693	931
	capacity Q	GWh	1.84	3.14
	$capex_{GHEs,pit}$	M€	1.55	1.74
Heat Pump	$\dot{Q}_{nom}$	kW	1227	1180
	$Q_{el,HP}$	GWh a^{-1}	1.31	0.42
	$capex_{HP}$	M€	2.35	1.40
Solar thermal field	$\dot{Q}_{nom,sol}$	kW	1054	2191
	module area	m^2	11329	23184
	$capex_{sol}$	M€	2.04	4.17

https://doi.org/10.52202/077185-0080

Table 1 gives an overview over additional techno-economic results regarding the storage systems and allows a comparison. $\dot{Q}_{\mathrm{nom}}$ denotes the nominal power of each component. $\dot{Q}_{\mathrm{nom,sol}}$ is the maximum power of the STC field fed into the grid and storage and not the nominally possible power of the field. The capex of the field $capex_{\mathrm{sol}}$ is calculated based on the module area, which might allow for higher heat flows in the summer being not necessary and thus not used. Both system configurations result in similar heat generation cost of about 22.5 ct $\mathrm{kW^{-1}h^{-1}}$. The total technological investments are higher for the PTES by around 19 %. This difference is mainly caused by the larger STC module area of the PTES case. The BTES field has a much smaller capacity than the PTES pit in terms of power and energy. Even though the specific capex both per kW and per GWh of the PTES is lower, the overall investments are higher compared to a BTES. This difference in size can, again, be explained with the conversion of much electricity in the BTES heat pump. Its electricity consumption $Q_{\mathrm{el,HP}}$ is three times higher than for the PTES heat pump. Consequently, this leads to high electricity costs and thus a high opex resulting in nearly the same heat generation costs for both systems even though the capex of a DHS with a PTES is higher. The capex of the BTES heat pump is substantially higher since the temperature difference which has to be overcome is much higher and a large heat pump with two stages has to be installed. The nominal power of the heat pump $\dot{Q}_{\mathrm{nom}}$ is in both cases approximately the same, since the same demand peaks have to be met. As mentioned above, the STC field of the PTES has roughly double the size compared to the BTES case. This is due to the low $Q_{\mathrm{el,HP,PTES}}$, the higher capacity Q_{PTES} and the losses associated with the PTES. With a reasonable initialization of the DHS and BTES model, the iterative optimization scheme does not lead to extensive simulation times but can be finished after only one loop taking less than three minutes time on a standard desktop PC, mainly caused by solving the DHS MILP model.

3.2 Sensitivity Analysis of the Electricity Price

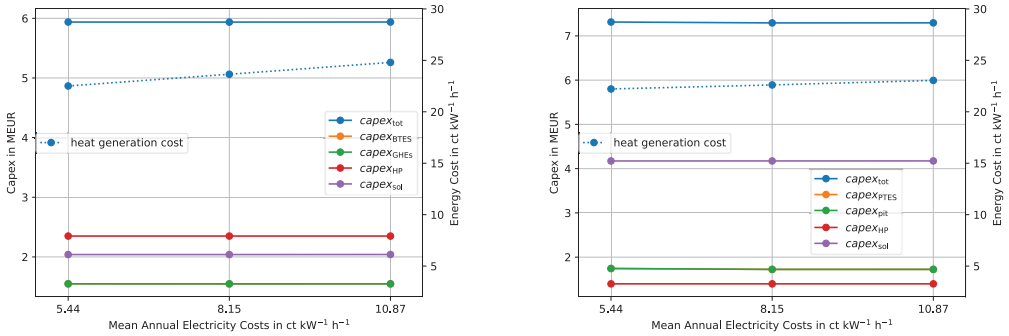

(a) (b)

Figure 3: Investment and energy costs over a varied electricity price for a DHS with (a) a BTES and (b) a PTES.

As shown in Table 1, the electricity price is a crucial parameter due to the role of $Q_{\mathrm{el,HP}}$. For a sensitivity analysis, the electricity price profile for 2030 has been multiplied by the constant factors 1, 1.5, and 2. In Figure 3, the annual mean of this profile is shown on the x-axis (with the baseline scenario from section 2.3 being 5.44 ct $\mathrm{kW^{-1}h^{-1}}$). On the left y-axis, the $capex$ as in Table 1, on the right y-axis the heat generation costs are plotted. For both technologies, the capex and therefore the dimension of the storage, heat pump and STC field remain constant with a changing electricity price. However, the heat generation costs increase linearly by 2.4 ct $\mathrm{kW^{-1}h^{-1}}$ over the entire interval in case of the BTES and by only 1.0 ct $\mathrm{kW^{-1}h^{-1}}$ for the PTES.

3.3 Sensitivity Analysis of the Thermal Conductivity λ_S of the Ground

Figure 4 (a) shows that a variation of λ_S has mainly a significant impact on the number of boreholes z needed for the GHE field. z decreases by about 42 % with an exponential behavior, the gradient

https://doi.org/10.52202/077185-0080

decreases for an increasing λ_S. The associated $capex_{\mathrm{GHEs}}$ decreases by 30 % (0.7 M€) exponentially as well. At the same time, the total investment costs $capex_{\mathrm{tot}}$ decrease by only 10 % and the heat generation costs by only 6 % from 24 ct $\mathrm{kW^{-1}h^{-1}}$ to 22.5 ct $\mathrm{kW^{-1}h^{-1}}$ due to the rather small share of $capex_{\mathrm{GHE}}$ of $capex_{\mathrm{tot}}$. The capex and dimensions of the STC field and the heat pump stay constant.

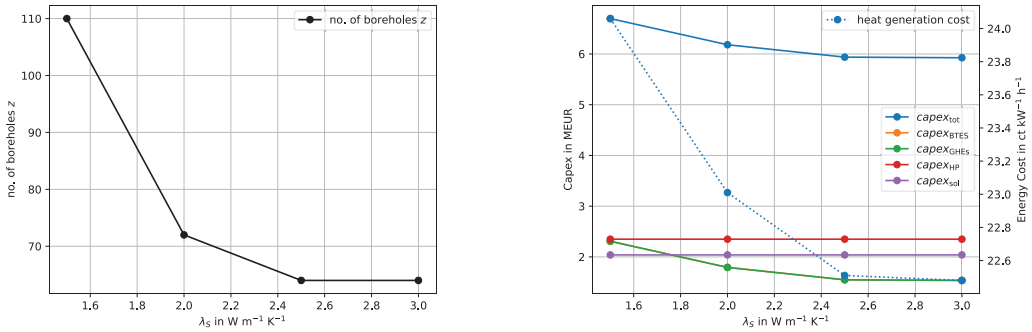

(a) (b)

Figure 4: (a) Number of required GHEs and (b) capex and heat generation cost over a varied thermal conductivity of the soil λ_S for a DHS with a BTES

3.4 Sensitivity Analysis of the Drilling and Land Area Costs

The specific drilling costs are another crucial parameter being already discussed in section 2.3. Figure 5 (a) plots the capex and heat generation costs over varied specific drilling costs c^{drill}. The linear dependencies lead to a linearly increasing $capex_{\mathrm{GHEs}}$ and heat generation costs with a gradient of about 2.75 ct $\mathrm{kW^{-1}h^{-1}}$ per $\Delta c^{\mathrm{drill}} = 100$ €$\mathrm{m^{-1}}$. As for λ_S, the capex and dimensions of the STC field and the heat pump stay constant and do not change with deteriorating conditions.

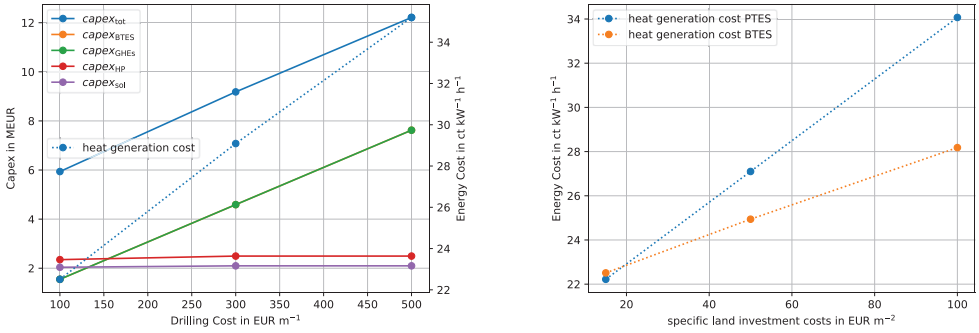

(a) (b)

Figure 5: (a) capex and heat generation costs over varied specific drilling costs c^{drill} for a DHS with a BTES and (b) heat generation costs over specific land investment costs c^{area} for a DHS with a BTES or a PTES

The specific land investment costs c^{area} are especially of importance regarding the land area costs for the STC field and the PTES. Most of the surface above the BTES can still be used. Therefore, the rise of the heat generation costs for a DHS with a BTES of 1.2 ct $\mathrm{kW^{-1}h^{-1}}$ per $\Delta c^{\mathrm{area}} = 20$ €$\mathrm{m^{-2}}$ in the given interval in Figure 5 (b) is mainly caused by the land costs for the STC field. The increase is much stronger for a PTES with 2.75 ct $\mathrm{kW^{-1}h^{-1}}$ per $\Delta c^{\mathrm{area}} = 20$ €$\mathrm{m^{-2}}$.

4 DISCUSSION

The method of the simplified storage model within the DHS MILP optimization model allows, if thoroughly initialized, even in the first run the consideration of the BTES characteristics when

https://doi.org/10.52202/077185-0080

optimizing a DHS. Furthermore, this approach enables to couple sophisticated and non-linear GHE simulation and optimization models like the *GHEDesigner* to the DHS MILP model optimizing large energy systems. This flexible approach facilitates the usage of different g-function models from *pygfunctions* (being used by *GHEDesigner*), allowing the simulation of different underground conditions, such as high groundwater flows. Even though for the time being, *GHEDesigner* is the open-source tool with the most functionalities regarding the optimization, any other tool could be coupled and used as well.

Regarding the comparison of BTES and PTES, the results show that the type of the long-term storage strongly determines the layout of the entire supply system. This is mainly caused by two effects: 1) The BTES with a balanced charging and discharging profile can compensate losses with geothermal gains which leads to a storage with "no losses". 2) The low COP of the BTES heat pump due to the high temperature difference between storage and grid leads to the conversion of much electricity into heat in the BTES heat pump. Compared to a DHS with a PTES, both effects allow smaller BTES storage capacities and STC field sizes.

However, BTES depend highly on the electricity price because of the high electric energy consumption of the BTES heat pump. These systems' costs are dominated by the opex, not the capex. Therefore, rising electricity costs in the future will lead to increased heat generation costs of DHS with BTES. The costs of DHS with PTES are much more stable regarding uncertainties in the electricity price prediction for the upcoming years. On the other hand, in configurations with rather low electricity prices or high electric energy potentials on-site, the BTES would turn even more advantageous. Clearly, this dependency caused by the low BTES COP might be slightly diminished in DHS with lower supply temperature like 4th or 5th generation DHS grids, which would lead to higher COP.

Even though the number of GHEs z and the associated $capex_{\mathrm{GHEs}}$ increase exponentially with a decreasing thermal conductivity of the soil λ_{S}, the change of the overall heat generation costs is rather small. Thus, on the one hand, uncertainties in λ_{S} at an early design stage are acceptable, and on the other hand, BTES can still be an economically very feasible solution even for rather low λ_{S}. Similar findings can be drawn from the results regarding the specific drilling costs c^{drill}. The, after all, rather moderate increases in the heat generation costs over the drilling costs c^{drill} ($2.75\ \mathrm{ct\,kW^{-1}h^{-1}}$ per $\Delta c^{\mathrm{drill}} = 100\ €\mathrm{m^{-1}}$) show that uncertainties regarding c^{drill} can be accepted at an early design stage.

The specific capex of a BTES (whether in $€\mathrm{kW^{-1}}$or $€\mathrm{kW^{-1}h^{-1}}$), being caused mainly by c^{drill}, is higher than for a PTES, aligning with the findings by Yang *et al.* (2021). But, taking the entire DHS into account, these lower specific costs of a PTES do not automatically make it the economically more feasible technology. Additionally, since BTES need less STC field area and the area above them can still be used, they are more advantageous in areas with high specific land investment costs c^{area} than PTES. Since BTES can be dimensioned with a much smaller capacity than PTES, they have a lower capex than PTES supplying the same grid with the same demand. Taking all costs into account, a DHS with a BTES can clearly compete with a DHS with a PTES.

5 LIMITATIONS OF RESULTS

The results are influenced by the temperature-dependent STC field efficiency $\mu_{k,t}$ from equation (5), being, in case of the BTES, determined by the grid temperature since the STC field has to supply the grid as well and not only the storage. For the BTES, the grid supply temperature is always higher than the storage temperature being rather low in the range of 30 °C due to optimal operation minimizing heat losses to the soil and regulatory requirements concerning soil and groundwater temperatures. The BTES could be charged at a much lower STC temperature leading to a higher $\mu_{k,t}$ leaving room for optimization of the BTES in the current model. Thus, it could perform even better than shown in the results applying an advanced control strategy. Regarding the PTES, its temperature can exceed the grid supply temperature and is generally high leaving only small optimization potential concerning $\mu_{k,t}$. Furthermore, the sensitivity analysis showed the strong influence of the land area costs being very low for BTES but not the PTES. Since rather low specific land area costs of $c^{\mathrm{area}} = 15\ €\mathrm{m^{-2}}$ are used in this case study, the BTES would show economically more feasible results in cases with higher c^{area} like in urban environments.

https://doi.org/10.52202/077185-0080

6 CONCLUSION AND OUTLOOK

This paper revealed and contributed to two main research gaps. 1) So far, the design optimization of BTES integrated in energy systems like DHS has mainly been focused on the GHE depth, and could not determine both the depth and the layout of the field. This can be overcome by combining a DHS MILP model including a simplified storage model and the GHE field optimization tool *GHEDesigner*. 2) The techno-economic performance of BTES compared to the competing PTES technology is still controversially discussed. A comparison of a DHS equipped with a STC field and a BTES or a PTES showed that both cases lead to similar heat generation costs of the overall system. BTES have higher specific capex but allow 41 % smaller storage capacity than PTES. This is possible, because BTES can compensate thermal losses with geothermal gains. Furthermore, due to low COP, the BTES heat pump converts much electric energy form the grid into heat. Both effects lead to a 51 % smaller STC area for BTES resulting in 19 % lower overall investment costs. But, the high electric energy consumption of the BTES heat pump being about three times higher leads to high opex and a strong dependency on the electricity price. While the BTES depends on the electricity price, the PTES is feasible mainly for low land area prices varying drastically between e.g., rural and urban areas. The assumption of a price of $c^{\mathrm{area}} = 100\ €\mathrm{m}^{-2}$ instead of $15\ €\mathrm{m}^{-2}$ leads to an increase in the PTES heat generation cost of 53 % while being only 25 % for the BTES. Since the drilling costs, being increased with the number of GHEs z, contribute rather little to the overall heat generation costs, BTES could be considered even for soil conditions with a rather low thermal conductivity λ_S.

In future work, the STC field model could be further refined to charge the BTES on a lower temperature level leading to higher STC efficiencies and further advantages of the BTES compared to the PTES, e.g., by varying the mass flow rate in the STC field or by splitting it up into two fields. Generally, prospective DHS will need lower supply temperatures making a BTES more favorable leading to both a higher COP and STC efficiency. The extent of these effects should be examined in further studies.

To conclude, the controversially led debate comparing BTES and PTES is legitimate and based on the strong dependencies on various parameters making it impossible to declare one of the two technologies as the generally economically more feasible. Regarding further seasonal storage developments, the combination of the concept of the simplified storage model in a DHS MILP model and an external complex or non-linear storage models seems very versatile and promising. This approach could be applied on other situations where a complex storage model like an aquifer storage has to be integrated into a techno-economic MILP DHS optimization tool.

REFERENCES

AGEB, 2016, *Anwendungsbilanzen für die Endenergiesektoren in Deutschland in den Jahren 2013 bis 2015: Studie beauftragt vom Bundesministerium für Wirtschaft und Energie, Projektnummer: 072/15*, Arbeitsgemeinschaft Energiebilanzen e.V.

Baehr, H.D. and Kabelac, S., 2006, *Thermodynamik: Grundlagen und technische Anwendungen mit zahlreichen Tabellen, Springer-Lehrbuch,* 13., neu bearbeitete und erweiterte Auflage, Springer-Verlag Berlin Heidelberg, Berlin, Germany.

Banks, D., 2015, Horatio Scott Carslaw and the origins of the well function and line source heat function, *SJG (Scottish Journal of Geology)*, Vol. 51 No. 1, pp. 100–104.

Beck, M., Bayer, P., Paly, M. de, Hecht-Méndez, J. and Zell, A., 2013, Geometric arrangement and operation mode adjustment in low-enthalpy geothermal borehole fields for heating, *Energy*, Vol. 49, pp. 434–443.

Blocon AB, 2022, *EED version 4: Update manual*, Lund, Sweden.

Blum, P., Campillo, G. and Kölbel, T., 2011, Techno-economic and spatial analysis of vertical ground source heat pump systems in Germany, *Energy*, Vol. 36 No. 5, pp. 3002–3011.

BMWK, 2019, *Energiedaten: Gesamtausgabe*, Berlin, Germany.

BMWK, 2021, *Energieeffizienz in Zahlen 2021: Entwicklungen und Trends in Deutschland 2021*.

Bordin, C., Gordini, A. and Vigo, D., 2016, An optimization approach for district heating strategic network design, *European Journal of Operational Research*, Vol. 252 No. 1, pp. 296–307.

https://doi.org/10.52202/077185-0080

Carslaw, H.S. and Jaeger, J.C., 1959, *Conduction Of Heat In Solids,* 2nd ed., Oxford University Press, London, Great Britain.
Cimmino, M. and Cook, J., 2022, Proceedings of the IGSHPA Research Track 2022, in *Proceedings of the IGSHPA Research Track 2022, 2022*, International Ground Source Heat Pump Association.
Connolly, D., Lund, H., Mathiesen, B.V., Werner, S., Möller, B., Persson, U., Boermans, T., Trier, D., Ostergaard, P.A. and Nielsen, S., 2014, Heat Roadmap Europe: Combining district heating with heat savings to decarbonise the EU energy system, *Energy Policy*, Vol. 65, pp. 475–489.
Danish Energy Agency, 2022, Technology Data, available at: https://ens.dk/en/our-services/projections-and-models/technology-data (accessed 19 May 2023).
ECB European Central Bank, 2024, Euro area bank interest rate statistics: December 2023, available at: https://www.ecb.europa.eu/press/stats/mfi/html/ecb.mir2402~882b313998.en.html (accessed 23 May 2024).
EED, 2019, *Tutorial: Examples for EED v4*, Lund, Sweden.
Eskilson, P., 1987 (1987), Thermal Analysis of Heat Extraction Boreholes, PhD Thesis, Department of Mathematical Physics, University of Lund, Lund, Sweden, 1987.
Eskilson, P. and Claesson, J., 1988, Simulation Model For Thermally Interacting Heat Extraction Boreholes, *Numerical Heat Transfer*, Vol. 13 No. 2, pp. 149–165.
European Commission, 2016, JRC Photovoltaic Geographical Information System (PVGIS)Interactive tools, available at: https://re.jrc.ec.europa.eu/pvg_tools/en/ (accessed 1 February 2023).
Florides, G.A., Christodoulides, P. and Pouloupatis, P., 2013, Single and double U-tube ground heat exchangers in multiple-layer substrates, *Applied Energy*, Vol. 102, pp. 364–373.
Gabrielli, P., Acquilino, A., Siri, S., Bracco, S., Sansavini, G. and Mazzotti, M., 2020, Optimization of low-carbon multi-energy systems with seasonal geothermal energy storage: The Anergy Grid of ETH Zurich, *Energy Conversion and Management: X*, Vol. 8, p. 100052.
Grünert, J., Kenkmann, T., Scheps, V., Pawlitzky, M., Scherf, B. and Ostin, A., 2009, *Nutzung von Erdwärme in Brandenburg: Heizen und Kühlen mit oberflächennaher Geothermie: Ein Leitfaden für Bauherren, Planer und Fachhandwerker,* 1st ed., Brandenburgische Energie Technologie Initiative (ETI), Potsdam, Germany.
Gurobi Optimization LL., 2023, *Gurobi Optimizer Reference Manual*.
Kotzur, L., Markewitz, P., Robinius, M. and Stolten, D., 2018, Time series aggregation for energy system design: Modeling seasonal storage, *Applied Energy*, Vol. 213, pp. 123–135.
Kümpel, A., Stoffel, P. and Müller, D., 2022, Development of a Long-Term Operational Optimization Model for a Building Energy System Supplied by a Geothermal Field, *J. Therm. Sci (Journal of thermal science)*, Vol. 31 No. 5, pp. 1293–1301.
Li, M. and Lai, A.C., 2015, Review of analytical models for heat transfer by vertical ground heat exchangers (GHEs): A perspective of time and space scales, *Applied Energy*, Vol. 151, pp. 178–191.
Lindsey, R. and Dahlmann, L., 2023, Climate Change: Global Temperature, available at: https://www.climate.gov/news-features/understanding-climate/climate-change-global-temperature (accessed 11 October 2023).
Lund, H., Möller, B., Mathiesen, B.V. and Dyrelund, A., 2010, The role of district heating in future renewable energy systems, *Energy*, Vol. 35 No. 3, pp. 1381–1390.
Mangold, D., Miedaner, O., Tziggili, E.P., Schmidt, T., Unterberger, M. and Zeh, B., 2012, *Technisch-wirtschaftliche Analyse und Weiterentwicklung der solaren Langzeit-Wärmespeicherung Forschungsbericht zum BMU-Vorhaben 0329607N*, Steinbeis Forschungsinstitut für solare und zukunftsfähige thermische Energiesysteme, Stuttgart, Germany.
McKenna, R., Fehrenbach, D. and Merkel, E., 2019, The role of seasonal thermal energy storage in increasing renewable heating shares: A techno-economic analysis for a typical residential district, *Energy and Buildings*, Vol. 187, pp. 38–49.
Paly, M. de, Hecht-Méndez, J., Beck, M., Blum, P., Zell, A. and Bayer, P., 2012, Optimization of energy extraction for closed shallow geothermal systems using linear programming, *Geothermics*, Vol. 43, pp. 57–65.

https://doi.org/10.52202/077185-0080

Peere, W. and Blanke, T., 2022, GHEtool: An open-source tool for borefield sizing in Python, *Journal of Open Source Software*, 7(76) No. 4406.

Pfluger, B., Hanßke, A., Ragwitz, M., Sporleder, M., Fritz, M., Kirbach, R., Ruscheinski, F., Steinbach, J., Popovski, E. and Haller, J., 2023, *Wissenschaftliche Transformationsstudie zur Dekarbonisierung der Wärmebereitstellung in der Region Hoyerswerda, Weißwasser und Spremberg bis 2050*, Fraunhofer-Gesellschaft.

Pinel, P., Cruickshank, C.A., Beausoleil-Morrison, I. and Wills, A., 2011, A review of available methods for seasonal storage of solar thermal energy in residential applications, *Renewable and Sustainable Energy Reviews*, Vol. 15 No. 7, pp. 3341–3359.

Robert, F. and Gosselin, L., 2014, New methodology to design ground coupled heat pump systems based on total cost minimization, *Applied Thermal Engineering*, Vol. 62 No. 2, pp. 481–491.

Schmidt, T., Mangold, D. and Müller-Steinhagen, H., 2004, Central solar heating plants with seasonal storage in Germany, *Solar Energy*, Vol. 76 No. 1, pp. 165–174.

Schmidt, T. and Sørensen, P.A., 2018, *Monitoring Results from Large Scale Heat storages for District Heating in Denmark*.

Schütz, T., Harb, H., Streblow, R. and Mueller, D., 2016, 28th International Conference on Efficiency, Cost, Optimization, Simulation and Environmental Impact of Energy Systems (ECOS 2015), in Bédécarrats, J.-P. (Ed.), *28th International Conference on Efficiency, Cost, Optimization, Simulation and Environmental Impact of Energy Systems (ECOS 2015), Pau, France, 30.06.-03.07.2015*, Curran Associates Inc, Red Hook, NY.

SenStadt, 2018, *Geothermisches Potenzial - spezifische Wärmeleitfähigkeit und spezifische Entzugsleistung (Ausgabe 2018)*, Berlin, Germany.

Spitler, J., West, T. and Liu, X., 2022, Proceedings of the IGSHPA Research Track 2022, in *Proceedings of the IGSHPA Research Track 2022, 2022*, International Ground Source Heat Pump Association.

Sporleder, M., Rath, M. and Ragwitz, M., 2024, Solar thermal vs. PV with a heat pump: A comparison of different charging technologies for seasonal storage systems in district heating networks, *Energy Conversion and Management: X*, Vol. 22, p. 100564.

Sporleder, M., Xu, Y., Rath, M., Ragwitz, M. and van Beek, M., 2023, 36th International Conference on Efficiency, Cost, Optimization, Simulation and Environmental Impact of Energy Systems (ECOS 2023), in Smith, J.R. (Ed.), *36th International Conference on Efficiency, Cost, Optimization, Simulation and Environmental Impact of Energy Systems (ECOS 2023), Las Palmas De Gran Canaria, Spain, 01.09.2020 - 05.09.2020*, ECOS 2023, Las Palmas De Gran Canaria, Spain, pp. 2241–2252.

UNFCCC, 2015, *Paris Agreement*.

VDI, 2010, *Thermal use of the underground: Fundamentals, approvals, environmental aspects No.* 4640, VDI Verein Deutscher Ingenieure, Berlin, Germany.

VDI, 2012, *Wirtschaftlichkeit gebäudetechnischer Anlagen: Grundlagen und Kostenberechnung* 2067 Blatt 1.

Welsch, B., 2019 (2019), Technical, Environmental and Economic Assessment of Medium Deep Borehole Thermal Energy Storage Systems, Dissertation, Department of Material and Earth Sciences, Technische Universität Darmstadt, Darmstadt, Germany, 2019.

Wirtz, M., Hahn, M., Schreiber, T. and Müller, D., 2021, Design optimization of multi-energy systems using mixed-integer linear programming: Which model complexity and level of detail is sufficient?, *Energy Conversion and Management*, Vol. 240, p. 114249.

Xiang, Y., Xie, Z., Furbo, S., Wang, D., Gao, M. and Fan, J., 2022, A comprehensive review on pit thermal energy storage: Technical elements, numerical approaches and recent applications, *Journal of Energy Storage*, Vol. 55, p. 105716.

Yang, T., Liu, W., Kramer, G.J. and Sun, Q., 2021, Seasonal thermal energy storage: A techno-economic literature review, *Renewable and Sustainable Energy Reviews*, Vol. 139, p. 110732.

ACKNOWLEDGEMENT

This research has been funded via the project ODH@Jülich.

https://doi.org/10.52202/077185-0080